

## Nuclear Structure of Na<sup>22</sup>. VI. Some Results for Levels with $E_{\text{ex}} > 2.9$ MeV\*

J. W. OLNESS, W. R. HARRIS, P. PAUL,<sup>†</sup> AND E. K. WARBURTON

*Brookhaven National Laboratory, Upton, New York 11973*

(Received 17 November 1969)

Further studies of the Ne<sup>20</sup>(He<sup>3</sup>, p)Na<sup>22</sup> reaction have been carried out to investigate in particular those Na<sup>22</sup> states of excitation energy greater than 2.9 MeV. From a measurement of the linear polarization of  $\gamma$  rays from Na<sup>22</sup> states formed in the above reaction, it has been determined that the 3-MeV doublet states at 2.969 MeV ( $J=3$ ) and 3.059 MeV ( $J=2$ ) both have even parity. The  $\gamma$  decays of higher-lying states were investigated through  $p$ - $\gamma$  coincidence measurements which utilized a 30-cc Ge(Li) spectrometer for  $\gamma$  detection. Correlation results lead to a  $J^\pi=3^-$  assignment for the 3.521-MeV state. The  $p$ - $\gamma$  measurements also determine the principal  $\gamma$  decay of 9 of the 13 states previously reported in the region 4 MeV  $< E_{\text{ex}} < 5.2$  MeV. Some information is also obtained on the spins of these states. Evidence is presented for the decay of a previously unreported level at an excitation energy of  $4.294 \pm 0.002$  MeV.

### I. INTRODUCTION

PREVIOUS studies of Na<sup>22</sup> have provided unique assignments of spin for 10 of the first 11 excited states of Na<sup>22</sup> reported<sup>1</sup> below  $E_{\text{ex}}=3.1$  MeV, and have also determined the parity of the first 9 of these levels. Figure 1 summarizes the available information<sup>2-10</sup> on spins, parities, and  $\gamma$ -ray branching ratios for the low-lying states of Na<sup>22</sup>. The branching ratios indicated in Fig. 1 for the states of  $E_{\text{ex}} < 4.1$  MeV incorporate the new results of the present experiment which have, in particular, determined the complex decay of the 3.52-MeV level and the principal decay of the 4.07-MeV level which had been previously only suggested.<sup>2,4,11</sup>

Prior measurements have also determined<sup>8,4,7,10,12-15</sup> (or set informative limits on) the mean lives of the levels with  $E_{\text{ex}} < 3.1$  MeV. The lifetimes of the levels at 0.657 and 1.937 MeV can also be inferred from

Mg<sup>22</sup> positron decay.<sup>16</sup> The measured lifetimes have been used, together with the branching-ratio information summarized in Fig. 1 and the previously measured mixing ratios,<sup>2-7,14</sup> to obtain dipole and quadrupole matrix elements for the transitions connecting these low-lying levels.<sup>6,7,14</sup>

As discussed previously,<sup>6,7,14</sup> the experimental description of the low-lying levels of Na<sup>22</sup> which emerges from the above investigations is qualitatively accounted for by either the rotational model or by a  $SU_3$  scheme. In particular, the prediction is that the lowest-lying levels shall be of even parity, arising from bands based on intrinsic states with  $(K, T) = (3, 0)$ ,  $(0, 0)$ , and  $(0, 1)$ .

The experimental description (summarized partially in Fig. 1) permits identification of the first 3 members of both the  $(3, 0)$  and  $(0, 1)$  bands, and probably the first 2 members of the  $(0, 0)$  band. Evidence has also been presented<sup>14</sup> for the tentative identification of a  $(K, T) = (1, 0)$  odd-parity band with a  $1^-, 2^-, 3^-, \dots$  level sequence, based on the experimental determination of odd parity for the states at 2.211 MeV ( $1^-$ ) and 2.572 MeV ( $2^-$ ). The most likely candidates for the  $J^\pi=3^-$  member of this band are the levels at 2.969 MeV ( $J=3$ ) and 3.521 MeV ( $J \geq 2$ ). It has been noted previously<sup>14</sup> that if one makes the identification of  $3^-$  with the 2.969-MeV state, then the 2.969  $\rightarrow$  1.952 transition ( $E1$ ) has a strength at least  $10^3$  times that of the  $\Delta T=1$  transitions from the  $1^-$  and  $2^-$  members of the band. This is in significant disagreement with the  $SU_3$  model which provides a marked inhibition of the  $\Delta T=1$   $E1$  decays.

In the light of this speculation, it is clear that an experimental determination of the spin and parity of the 2.969- and 3.521-MeV levels is of particular importance to the collective-model considerations of Na<sup>22</sup>. Additional information on the character of higher-lying states is also desirable, in that it would hopefully permit an identification of the higher-spin members of the even-parity bands.

<sup>16</sup> A. Gallmann, G. Frick, E. K. Warburton, D. E. Alburger, and S. Hecht, Phys. Rev. **163**, 1190 (1967).

\* Work performed under the auspices of the U.S. Atomic Energy Commission.

<sup>†</sup> Guest physicist from State University of New York at Stony Brook, Stony Brook, N.Y.

<sup>1</sup> S. Hinds, H. Marchant, and R. Middleton, Nucl. Phys. **51**, 427 (1964).

<sup>2</sup> H. J. Maier, P. Pelte, J. G. Pronko, and C. Rolfs, Nucl. Phys. **84**, 1 (1966).

<sup>3</sup> E. K. Warburton, J. W. Olness, and A. R. Poletti, Phys. Rev. **160**, 938 (1967).

<sup>4</sup> A. R. Poletti, E. K. Warburton, J. W. Olness, and S. Hecht, Phys. Rev. **162**, 1040 (1967).

<sup>5</sup> A. R. Poletti, E. K. Warburton, and J. W. Olness, Phys. Rev. **164**, 1479 (1967).

<sup>6</sup> E. K. Warburton, A. R. Poletti, and J. W. Olness, Phys. Rev. **168**, 1232 (1968).

<sup>7</sup> J. G. Pronko, C. Rolfs, and H. J. Maier, Phys. Rev. **167**, 1066 (1968).

<sup>8</sup> T. Wei, Bull. Am. Phys. Soc. **13**, 85 (1968); (private communication).

<sup>9</sup> R. C. Haight, thesis, Princeton University, 1969 (unpublished).

<sup>10</sup> E. K. Warburton, L. E. Carlson, G. T. Garvey, D. A. Hutcheon, and K. P. Jackson, Nucl. Phys. **A136**, 160 (1969).

<sup>11</sup> S. E. Arnell and E. Wernborn-Selin, Arkiv Fysik **27**, 1 (1964).

<sup>12</sup> A. E. Blaugrund, A. Fischer, and A. Z. Schwarzschild, Nucl. Phys. **A107**, 411 (1968).

<sup>13</sup> K. W. Jones, A. Z. Schwarzschild, E. K. Warburton, and D. B. Fossan, Phys. Rev. **178**, 1773 (1969).

<sup>14</sup> P. Paul, J. W. Olness, and E. K. Warburton, Phys. Rev. **173**, 1063 (1968).

<sup>15</sup> R. W. Kavanagh, Bull. Am. Phys. Soc. **12**, 913 (1967).



The true experimental polarization is related to  $S(\theta)$  by

$$P(\theta) = S(\theta)/Q, \quad (5)$$

where  $Q$  is a constant (i.e., independent of  $\theta$ ) which expresses the energy dependence of the Compton scattering process, and contains specifically the geometrical factors of the actual polarimeter. Note in Eq. (5) that  $P(\theta)$ , and also  $S(\theta)$  and  $Q$ , may be either positive or negative. An experimental measurement of  $P(90^\circ)$ , defined by Eq. (5), can be compared to that predicted for different multipoles by Eq. (2) to distinguish between electric and magnetic dipole radiation, provided the angular distribution of Eq. (1) can be specified from an independent or concurrent measurement.

### B. Experiment

The  $\text{Ne}^{20}(\text{He}^3, p)\text{Na}^{22}$  reaction was initiated by bombardment of a natural neon (90.92%  $\text{Ne}^{20}$ ) gas target using the  $\text{He}^{3++}$  beam from the BNL Van de Graaff accelerator at a bombarding energy of 6.92 MeV. The target gas was constrained in a cylindrical target cell at a pressure of 0.5 atm by entrance and exit windows of 0.1-mil Ni foil. The target cell was located at the center of an 8-in.-diam scattering chamber. An annular surface-barrier detector was positioned at  $180^\circ$  relative to the beam direction, set to detect charged particles emanating from the target cell within the angular range  $168^\circ \leq \theta_p \leq 172^\circ$ . The three-crystal polarimeter was mounted on a correlation table which could be moved in the range  $0 \leq \theta_\gamma \leq 90^\circ$ , and was actually set at  $\theta_\gamma = 90^\circ$  since the polarization is maximum there for dipole radiation.

For these measurements the  $\gamma$ -ray spectra observed with the polarimeter were measured in coincidence with the protons leading to the 3-MeV doublet levels, using a single voltage gate set on the 2.97- and 3.06-MeV proton groups which were unresolved by the particle detector. The above coincidence condition served two purposes: (1) The resultant  $\gamma$ -ray spectrum viewed by the polarimeter contained only the deexcitation  $\gamma$  rays from the 2.97- and 3.06-MeV levels. (2) The colinear particle detection scheme restricts the population of the initial levels ( $J=2$  or  $3$ ) to the magnetic substates  $m=0$  or  $\pm 1$ , and thus the initial states are aligned.

The polarimeter itself consisted of a central  $1 \times 3$ -in. NaI(Tl) scattering crystal, and two  $3 \times 3$ -in. NaI(Tl) side detectors, whose relative positions were fixed by machined aluminum holders. The central crystal was located with its axis along the direction of the incident  $\gamma$ -ray flux. The two side detectors were positioned at right angles to this direction, with one detector located in the reaction plane ("parallel" detector) and the other located in the plane normal to the reaction plane ("perpendicular" detector).

Time-coincident pulses from the scattering and "parallel" detectors, corresponding to a given Compton scattering event, were summed by an adding circuit

before presentation to one of two identical 1024-channel analyzers. The analyzer was gated by a fast-slow coincidence circuit which signaled that a particular "in-plane" scattering event had taken place. In addition to requiring a simultaneous input from the particle detector gate, the coincidence circuit imposed a voltage gate on the pulses from the "parallel" detector covering the energy range 380–540 keV. This corresponds to a restriction on the Compton scattering angle of roughly  $60^\circ$ – $90^\circ$ . An identical system was used for the simultaneous analysis of pulses corresponding to scattering into the "perpendicular" detector.

Figure 2 shows the coincidence spectra thus measured with the polarimeter, each labeled according to whether the scattering took place into the "parallel" or "perpendicular" detectors. Here we see the three  $\gamma$  rays resulting from the  $2.97 \rightarrow 1.95 \rightarrow 0.58$  and  $3.06 \rightarrow 1.95 \rightarrow 0.58$  transitions, where the  $1.95 \rightarrow 0.58$  peak represents the sum of the separate contributions from the two cascade routes. From inspection of Fig. 2, it is apparent that the relative peak areas measured for the  $2.97 \rightarrow 1.95$  transition are markedly different, as are those also for the  $3.06 \rightarrow 1.95$  transition, indicating an azimuthal asymmetry in the Compton scattering process corresponding to a measureable polarization. For each spectrum the peak areas were determined using a least-squares computer fit to the data, in which the data were represented as the sum of three Gaussian peaks superimposed on a smooth background. The values of  $Y_\perp$  and  $Y_\parallel$  thus determined were then used to compute the quantity  $S(90^\circ)$  which is tabulated in Table I. The experimental polarizations  $P(90^\circ) = S(90^\circ)/Q$  are also shown, where we have used for the calibration constant,  $Q$ , values computed from the relationship established previously<sup>5</sup> for this polarimeter, namely,

$$Q = (0.340 \pm 0.053) - (0.079 \pm 0.035) E_\gamma,$$

where  $E_\gamma$  is in MeV. Since the polarimeter is as nearly as possible identical to that used previously, it is expected that the above relationship holds also for the present measurement. This was checked by independent measurements on the  $2.21 \rightarrow 0.66$  transition, as we shall illustrate later.

The angular distribution coefficients were measured under identical experimental conditions, but with a  $3 \times 3$ -in. NaI(Tl) detector (polarization insensitive) replacing the three-crystal polarimeter. Previous work<sup>4,6</sup> had shown that the 2.97- and 3.06-MeV levels decay to the 1.95-MeV level by predominantly dipole transitions such that the angular distributions have  $a_2$  terms only, with negligible  $a_4$  terms. From an analysis of the spectra obtained at detector angles  $\theta_\gamma = 0^\circ$  and  $90^\circ$ , measured in coincidence with protons leading to the 2.97- and 3.06-MeV levels, the areas under the full energy peaks were determined. The results were then fitted to determine the coefficients  $a_2$ . The values summarized in Table I are an average of the present results with previous<sup>4</sup> results obtained under identical circum-

TABLE I. Experimental results obtained for the linear polarization of  $\gamma$  rays from various states in  $\text{Na}^{22}$  observed at  $\theta_\gamma=90^\circ$ . The measured quantities  $a_2$  and  $S(90^\circ)$  lead to the experimental and predicted polarizations  $P(90^\circ)$  as explained in the text.  $P(90^\circ)_{\text{theor}}$  is the prediction for pure dipole radiation with the multipolarity chosen to give agreement in sign with experiment.

Transition (MeV)	$a_2$	$S(90^\circ)$	$E_\gamma$ (MeV)	$P(90^\circ)_{\text{expt}}$	$P(90^\circ)_{\text{theor}}$	Multiplicity
2.211 $\rightarrow$ 0.657	$-0.76 \pm 0.03$	$-0.26 \pm 0.06$	1.554	$+1.17 \pm 0.34$	$+0.82 \pm 0.03$	E1
2.969 $\rightarrow$ 1.952	$-0.37 \pm 0.11$	$+0.26 \pm 0.06$	1.017	$-1.01 \pm 0.34$	$-0.47 \pm 0.05$	M1
3.059 $\rightarrow$ 1.952	$+0.21 \pm 0.05$	$-0.16 \pm 0.04$	1.107	$+0.61 \pm 0.21$	$+0.35 \pm 0.07$	M1
1.952 $\rightarrow$ 0.583	$-0.22 \pm 0.05$	$+0.07 \pm 0.02$	1.369	$-0.30 \pm 0.12$	$-0.30 \pm 0.06$	M1

stances. The predicted polarizations computed from Eq. (2) for pure dipole radiation, corresponding to these values of  $a_2$ , are summarized in column 6 of Table I. Here we have chosen the sign to agree with the measured polarization; the character of the dipole radiation corresponding to the sign chosen is given in column 7. This comparison indicates that both transitions are

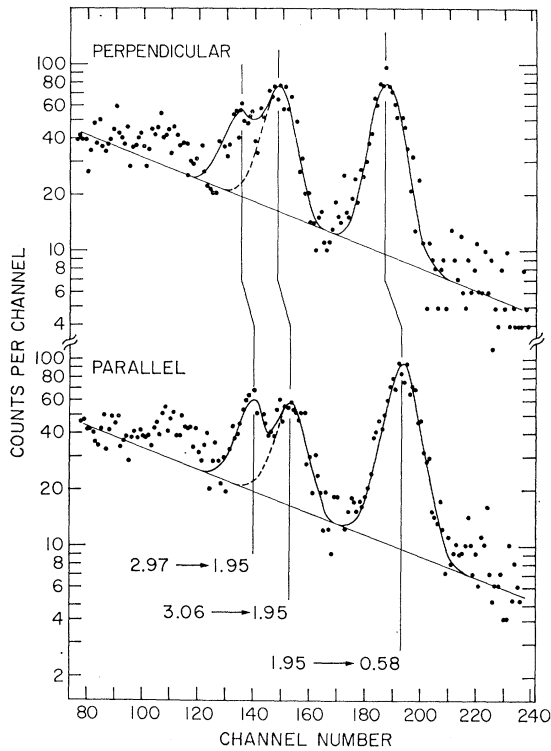


FIG. 2. Spectra of  $\gamma$  rays from the  $\text{Ne}^{20}(\text{He}^3, p)\text{Na}^{22}$  reaction measured by a three-crystal  $\text{NaI}(\text{Tl})$  Compton polarimeter at  $\theta_\gamma=90^\circ$  relative to the incident  $\text{He}^3$  beam direction. These data were measured in coincidence with protons leading to the 2.97- and 3.06-MeV levels, detected by an annular Si detector centered at  $\theta_p=180^\circ$ . From the relative areas of the observed peaks, which correspond to the probability for Compton scattering in the planes "parallel" and "perpendicular" to the reaction plane (defined by the polarimeter), the linear polarizations of the 2.97 $\rightarrow$ 1.95 and 3.06 $\rightarrow$ 1.95 transitions were obtained. As explained in the text, the measured polarizations show that both transitions are M1 in character. The data on the 1.95 $\rightarrow$ 0.58 transition, which represents the sum of the secondary members of the above cascades, provided one of the checks on the polarimeter efficiency.

M1. However, since small admixtures of quadrupole radiation are possible in both transitions we must consider the effects of these admixtures using Eq. (3). The result is illustrated in Fig. 3 which shows the theoretical polarization of Eqs. (2) and (3) calculated using the  $a_2$  coefficients of Table I. Also shown are the allowed values of the mixing ratios of the two transitions<sup>4,6</sup> and the measured  $P(90^\circ)$ . We conclude that there is no parity change involved in the 2.97 $\rightarrow$ 1.95 and 3.06 $\rightarrow$ 1.95 transitions leading to the even-parity 1.95-MeV level, and thus both the 2.97- and 3.06-MeV levels must also be of even parity.

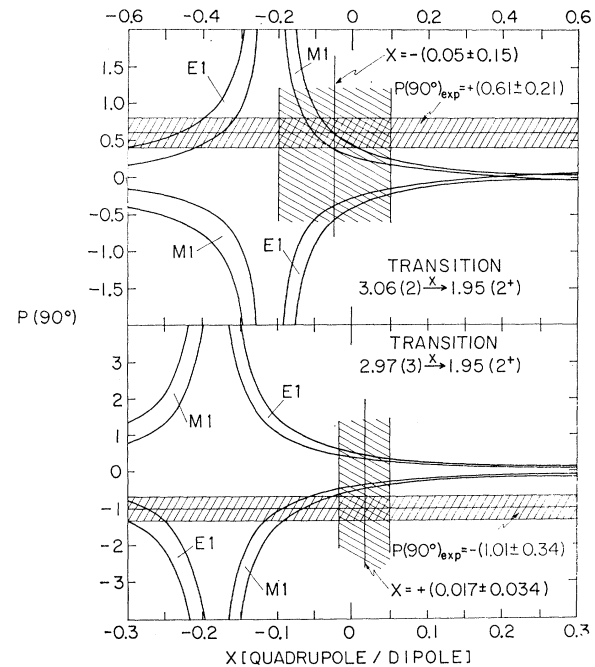


FIG. 3. Linear polarization  $P(90^\circ)$  as a function of the quadrupole-dipole mixing ratio  $x$  for the  $\gamma$ -ray transitions indicated. The theoretical curves were calculated using Eq. (2). Curves are shown for values of  $a_2$  one standard deviation either way from the mean (Table I). Experimental values of  $P(90^\circ)$  are also shown as well as the region of  $x$  allowed by previous work (Refs. 4 and 6). For the 3.06 $\rightarrow$ 1.95 transition, the indicated lower limit on  $x$  is roughly the 0.1% confidence limit. The "correct" theoretical curve lies within the intersection of the cross-hatched regions indicating the experimentally allowed regions of  $P(\theta)$  and  $x$ .

Also shown in Table I are the values of  $S(90^\circ)$  and correspondingly  $P(90^\circ)$  obtained from the above data for the  $1.95 \rightarrow 0.58$  transition, which results from feeding of the 1.95-MeV level via cascades from the 3-MeV doublet levels. It has been previously shown<sup>6</sup> that the  $1.95(2^+) \rightarrow 0.58(1^+)$  transition is primarily dipole, the restriction on possible quadrupole mixing being given by  $x = +(0.04 \pm 0.06)$ . As can be seen from Table I, the predicted polarization calculated from Eq. (2), based on the measured value of the distribution coefficient  $a_2$ , is in good agreement with the experimental polarization if we choose the sign to agree with  $M1$  character for the  $1.95 \rightarrow 0.58$  transition, as it must be. As an additional check, the polarization of  $\gamma$  rays from the  $2.21(1^-) \rightarrow 0.66(0^+)$  transition was measured in a separate experiment. Again, the  $\gamma$  rays were observed in coincidence with the protons leading to the 2.21-MeV state. Table I summarizes the values of  $S(90^\circ)$  and  $P(90^\circ)$  thus determined, together with the theoretical polarization predicted from the value of  $a_2$ . As can be seen, the predicted and measured polarizations agree very well if we choose the  $+$  sign in Eq. (2). This corresponds to  $E1$  radiation, in agreement with the previous conclusions which have determined that this is a  $1^- \rightarrow 0^+$  transition.

### III. BRANCHING RATIO AND CORRELATION MEASUREMENTS

#### A. Ge(Li) Measurements

##### Method

Proton- $\gamma$  coincidence spectra from the  $\text{Ne}^{20}(\text{He}^3, p\gamma)\text{Na}^{22}$  reaction were measured using a 5-in.-diam chamber<sup>20</sup> which permitted colinear detection of the reaction protons. The target gas of natural neon was constrained at a pressure of 0.33 atm in a 0.6-cm-long target cell which was located at the center of the chamber. The charged particles resulting from  $\text{He}^{3++}$  bombardment of the target cell were detected by an annular surface-barrier detector, placed concentric with the beam axis and subtending an angle defined by  $165^\circ \leq \theta_p \leq 175^\circ$ . A 6.85-mg/cm<sup>2</sup> Al absorber was placed over the front face of the detector to stop elastically scattered  $\text{He}^3$  particles, and the detector was additionally shielded against electrons emanating from the target cell by a small ferrite magnet ( $\sim 400$  G/cm<sup>2</sup>) placed between the target and detector.  $\gamma$  rays were detected with a coaxial 30-cm<sup>3</sup> Ge(Li) detector located with its front face at a distance of 7 cm from the target cell. The  $\gamma$  detector system utilized pole-zero amplification and dc restoration in order to achieve resolutions of  $\leq 3$  keV at count rates of up to  $5 \times 10^4$  counts/sec. With the indicated geometry, the  $\gamma$  detector subtended a solid

angle of 1.2% of a sphere, and correspondingly the particle detector subtended 1.5% of a sphere.

The time-coincidence spectrum of pulses from the detectors was analyzed by a TMC 16 384-channel analyzer, set to operate in a  $512(\gamma) \times 32(\text{proton})$ -channel mode. The analyzer was gated on by an external coincidence circuit of resolving time  $2\tau = 60$  nsec. Two separate measurements were carried out in order to investigate the  $\gamma$  decay of states of interest:

(1) In the first, the particle detector system was set to display protons corresponding to the range of excitation energies in  $\text{Na}^{22}$  of  $2.4 < E_{\text{ex}} < 4.1$  MeV. The range of  $\gamma$  analysis was approximately  $0.4 < E_\gamma < 3.8$  MeV, which included the second escape peaks of all possible ground-state transitions. This measurement was made at a bombarding energy of  $E_{\text{He}^3} = 6.9$  MeV, corresponding to an energy incident on the  $\text{Ne}^{20}$  gas target of 6.1 MeV. Coincidence data were recorded at each of three angles  $\theta_\gamma = 37^\circ, 55^\circ,$  and  $90^\circ$ , for a total running time of 80 h, corresponding to a net bombardment of 0.0147 C. (The design of the chamber precluded measurements for  $\theta_\gamma < 37^\circ$ .) The results, which will be discussed later, established the decay of the 3.52-MeV level (previously known<sup>2,4</sup> to be complex) and confirmed the previously reported<sup>4,6</sup> branching of the states at 2.572, 2.979, 3.059, and 3.947 MeV.

(2) For the second measurement, the range of analysis was modified to study the  $\gamma$  decay of  $\text{Na}^{22}$  states in the range  $3.4 < E_{\text{ex}} < 5.2$  MeV. A bombarding energy of  $E_{\text{He}^3} = 5.81$  MeV was used, corresponding to an

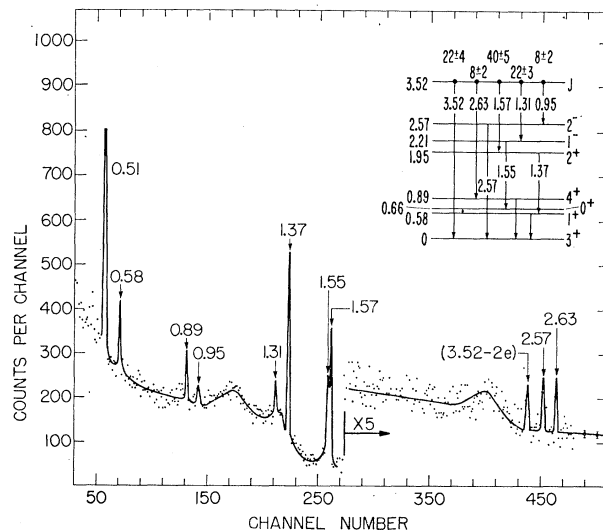


FIG. 4. Spectra of  $\gamma$  rays from the  $\text{Ne}^{20}(\text{He}^3, p\gamma)\text{Na}^{22}$  reaction measured in coincidence with protons leading to the 3.52-MeV state of  $\text{Na}^{22}$ . These data were measured with a 30-cc Ge(Li) detector at  $\theta_\gamma = 90^\circ$ ; the annular particle detector was centered at  $\theta_p = 180^\circ$ . The various lines are identified by the transition energies and have been fitted into the  $\text{Na}^{22}$  level scheme as shown in the inset. From similar data obtained at  $\theta_\gamma = 55^\circ$  and  $37^\circ$ ,  $p$ - $\gamma$  angular correlation data were extracted and used to determine the relative transition intensities, resulting in the branching ratios quoted in the inset.

<sup>20</sup> J. W. Olness and E. K. Warburton, Phys. Rev. **151**, 792 (1966).

TABLE II. Summary of angular correlation results for the 3.52-MeV level of  $\text{Na}^{22}$ .

Transition	$W(\theta)$ (arbitrary units)			Restrictions on $x$ , $(L+1)/L$ mixing in primary transition			
	$\theta=90^\circ$	$\theta=55^\circ$	$\theta=37^\circ$	$J_i=2$		$J_i=3$	
				$x$	$\chi^2$	$x$	$\chi^2$
3.52→0	29±9	52±16	86±17	+0.23≤ $x$ ≤+2.48	2.9	-11.43≤ $x$ ≤+0.32	0.6
3.52→0.89	30±9	65±17	26±13	no restriction	...	no restriction	...
3.52→1.95	396±65	374±22	280±12	+0.49≤ $x_1$ ≤+1.88	1.6	-0.12≤ $x_1$ ≤+0.27	0.5
1.95→0.58	507±25	425±35	360±36	$x_2 \equiv + (0.04 \pm 0.06)$		$x_2 \equiv + (0.04 \pm 0.06)$	
3.52→2.21	95±19	297±38	341±42	no solution	4.6	-0.16≤ $x_1$ ≤+0.90	1.0
2.21→0.66	290±36	170±21	160±13	$x_2 \equiv 0$		$x_2 \equiv 0$	
3.52→2.57	64±23	68±32	210±42	-3.27≤ $x$ ≤+0.09	3.6	-5.14≤ $x$ ≤-0.38	1.8

energy incident on the  $\text{Ne}^{20}$  target gas of 5.06 MeV. Data were acquired over a period of 50 h at angles  $\theta_\gamma = 37^\circ, 55^\circ$ , and  $90^\circ$ , for a net bombardment of 0.010 C.

The analysis of the two-parameter data for levels of  $E_{\text{ex}} < 4.1$  MeV was carried out in a fashion described previously.<sup>20</sup> Since the particle detector was capable of resolving all of the states of interest, the  $\gamma$  spectrum measured in coincidence with a particular proton group was easily extracted from the two-parameter matrix. As an example, Fig. 4 shows the Ge(Li) spectrum measured in coincidence with proton  $p_{12}(3.52)$  leading to the 3.52-MeV state of  $\text{Na}^{22}$ . The lines are identified by their energies (nominal) and lead to the decay scheme shown in the insert. Similar plots were constructed for the remaining levels of  $2.4 < E_{\text{ex}} < 4.1$  MeV. The results we shall summarize briefly.

#### Results for the Lower-Lying States

*Levels of  $E_{\text{ex}} < 3.1$  MeV.* The results obtained from the data for  $E_{\text{He}^3} = 6.9$  MeV essentially confirm the previously quoted branching for several of the states below  $E_{\text{ex}} = 3.1$  MeV. The 2.57-MeV level was observed to deexcite to the ground state and first excited state with branches of  $80 \pm 5\%$  and  $20 \pm 5\%$ , respectively, in excellent agreement with the previously quoted values<sup>4</sup> of  $81 \pm 3\%$  and  $19 \pm 3\%$ . The 2.97- and 3.06-MeV levels both cascade through the 1.952-MeV level, these being the only transitions observed. The correlation data for these three states are in qualitative agreement with that obtained previously,<sup>4,6,14</sup> but were not analyzed.

*The 3.52-MeV Level.* The spectrum of  $\gamma$  rays measured with the Ge(Li) detector in coincidence with protons leaving  $\text{Na}^{22}$  in its 3.52-MeV (12th excited) state is shown in Fig. 4. This spectrum was obtained from the two-parameter data for  $\theta_\gamma = 90^\circ$ , measured at  $E_{\text{He}^3} = 6.9$  MeV. The strongest lines in the spectra, as obtained at this angle and also at the remaining two correlation angles, were those at 1.57 and 1.37 MeV from the 3.52→1.95→0.58 cascade, and those at 1.31 and 1.55 MeV resulting from the 3.52→2.21→0.66 cascade. The second escape peak of the 3.52→0 transition is also evident at  $(3.52 - 1.02) = 2.50$  MeV. The less intense

lines at 0.95 and 2.57 MeV result from the 3.52→2.57→0 cascade, while those at 2.63 and 0.891 MeV are from the 3.52→0.891→0 cascade. These conclusions are supported by the data obtained for  $\theta_\gamma = 55^\circ$  and  $37^\circ$ .

The energies of each transition are based on an internal calibration utilizing the known energies of other lines in the two-parameter data matrix, and result in an excitation energy for this level of  $3521 \pm 2$  keV. This is in agreement with the previous value<sup>1</sup> of  $3527 \pm 10$  keV.

For each of the lines evident in Fig. 4, the intensity was extracted for each of the three angles of observation, and normalized according to the current integrator. These results were next fitted with an even-order Legendre polynomial in order to determine the relative intensity of each line. The branching ratios thus deduced are shown in the inset of Fig. 4. In these calculations, the relative peak efficiency of the 30-cc Ge(Li) detector was taken, as a function of  $E_\gamma$ , from an extrapolated curve based on similar detectors with volumes in the range 25–40 cc. The branching ratios summarized in Fig. 4 are in excellent agreement with the information gotten previously<sup>4</sup> with NaI(Tl) spectroscopy. For example, the previous value of  $18 \pm 6\%$  for the ground-state branch agrees well with the value given of  $22 \pm 4\%$ . The net intensity of the unresolved 3.52→0.89 and 3.25→2.57 branches was  $15 \pm 5\%$ , while the unresolved 3.52→(2.21+1.95) branch was quoted as  $67 \pm 5\%$ , again in very good agreement.

These measurements also provide a useful limit on the mean life of the 3.52-MeV level. Detection of the reaction protons in a backward direction insures that the excited recoiling  $\text{Na}^{22}$  ions have a large initial velocity ( $v_R/c = 1.43\%$ ) along the beam axis (i.e.,  $\cos\theta_R \approx 1$ ). All of the transitions from the 3.52-MeV level do, in fact, exhibit Doppler shifts for the detection angles  $\theta_\gamma = 55^\circ$  and  $37^\circ$ . Since the Doppler shift is linear in  $\cos\theta$ , the data were easily fitted to obtain the  $0^\circ$ – $90^\circ$  shift for the second escape peak of the 3.52→0 transition, yielding a value  $\Delta E_{\text{expt}} = 51 \pm 4$  keV. The expected kinematic shift for a very short lifetime is

$$\Delta E_K = E_\gamma [1 + (v_R/c) \cos\theta_R] = 50 \text{ keV.}$$

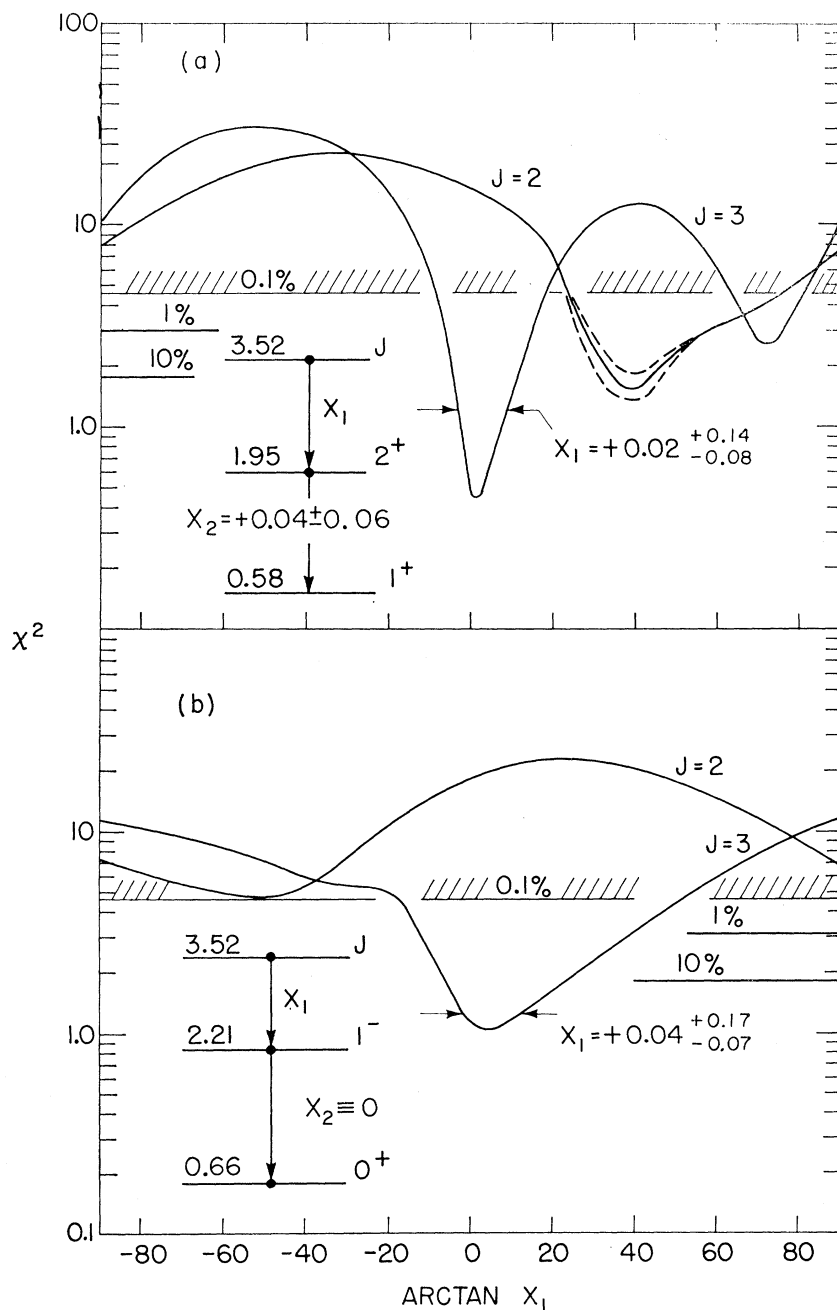


FIG. 5. Partial results of a  $\chi^2$  analysis of the  $p$ - $\gamma$  angular correlation data obtained for the major transitions from the  $\text{Na}^{22}$  3.52-MeV level. In plots (a) and (b) we have illustrated the results of a simultaneous fit to the data for the  $3.52 \rightarrow 1.95 \rightarrow 0.58$  and  $3.52 \rightarrow 2.21 \rightarrow 0.66$  cascade transitions, respectively. In each case, the goodness-of-fit parameter  $\chi^2$  is plotted as a function of  $x_1$ , the  $(L+1)/L$  mixing in the primary cascade. The mixing in the secondary member has been restricted, as indicated, on the basis of previously available information as given in the text. The explicit parameters of the fit are the population parameters  $P(0)$  and  $P(1)$  which describe the alignment of the initial state. Finite size effects have been accounted for by allowing a small admixture of the  $P(2)$  substate population.  $\chi^2$  is normalized, so that its expectation value is unity; the 10, 1, and 0.1% confidence limits are indicated. Results are shown for assumed spins of  $J=2$  and 3 for the 3.52-MeV level. Other possible spin assignments have been eliminated from a number of considerations enumerated in the text. As illustrated, only  $J=3$  is consistent with both sets of data. The corresponding solutions for  $x$ , taken at one standard deviation, are indicated. Note that the dashed lines in (a) illustrate the effects for  $J=2$  of varying  $x_2$  within the indicated limits; for  $J=3$  the effects are negligible.

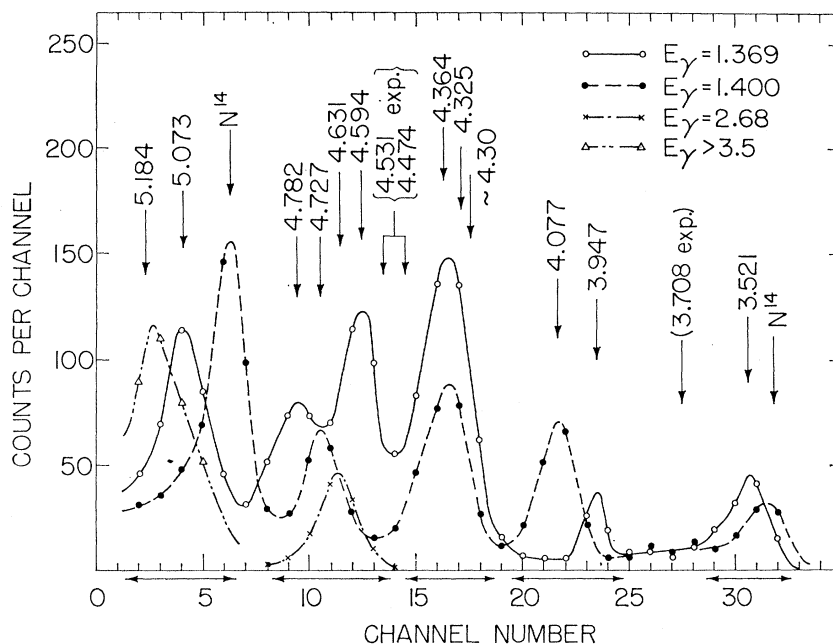
We thus obtain an attenuation factor

$$F'(\tau) = E(0^\circ-90^\circ)_{\text{expt}}/\Delta E_K = 1.01 \pm 0.07.$$

A value for  $F'(\tau)$  may also be extracted from the  $2.57 \rightarrow 0$  transition, since the mean life of the 2.57-MeV level is known<sup>14</sup> to be much shorter than the limit we will extract in this manner. This was done (independently for  $\theta_\gamma = 55^\circ$  and  $37^\circ$ ) by observing that the peak position of the  $2.57 \rightarrow 0$  transition measured in coincidence with proton group  $p_{12}$  (3.52-MeV level) was not measurably shifted from that observed in coincidence with

proton group  $p_9$  (2.57-MeV level). In the latter case, the  $2.57 \rightarrow 0$  transition experiences the full Doppler shift. Since these data were all within the same data matrix, uncertainties in the energy calibration are not of any significance here. The restriction on  $F'(\tau)$  from this comparison is  $F'(\tau) = 1.04 \pm 0.07$ . The average of these two values is  $F'(\tau) = 1.02 \pm 0.05$ . Using the value for the characteristic stopping time,  $\alpha = 750$  psec, appropriate to  $\text{Ne}^{20}$  gas at 0.33 atm, the above average value for  $F'(\tau)$  leads to an upper limit on the mean life for the 3.52-MeV level of  $\tau < 60$  psec, where we have

FIG. 6. Partial results of a two-parameter analysis of  $p$ - $\gamma$  coincidences in the  $\text{Ne}^{20}(\text{He}^3, p\gamma)\text{Na}^{22}$  reaction measured at  $E_{\text{He}^3}=5.1$  MeV. The plots show the proton spectra observed with an annular detector set at  $\theta_p=180^\circ$ , measured in coincidence with specific  $\gamma$ -ray lines characterizing the deexcitation of various states of  $\text{Na}^{22}$ . The  $\gamma$  rays were detected by a 30-cc Ge(Li) detector set at  $\theta=55^\circ$ . The expected positions of particular proton groups are indicated by the arrows and labeled by the level excitation energies in MeV. Evidence is also obtained for a previously unreported state in  $\text{Na}^{22}$  at  $E_{\text{ex}}=4.30$  MeV. The decay scheme of these  $\text{Na}^{22}$  levels was determined from the Ge(Li) spectra measured in coincidence with specific proton groups.



allowed for 2 standard deviations in the measured  $F'(\tau)$ .

The possibilities  $J=0$  and  $J\geq 4$  for the spin of the initial 3.52-MeV level are eliminated by the lifetime limit since the de-excitation transitions (see Fig. 4) to the  $J^\pi=4^+$  0.89-MeV level (for  $J=0$ ) and the  $J^\pi=1^-$  2.21-MeV level (for  $J\geq 4$ ) would be prohibitively strong. An assignment of  $J=1$  is also ruled against by the lifetime limit since the  $3.52\rightarrow 0.89$  transition, if  $E3$ , would have a strength of at least 55 Weisskopf units<sup>21</sup> (corresponding to a lower limit on the branching ratio of 4%). In addition, the possibilities  $J=0, 1$ , and 4 are excluded by the correlation information on the major transitions to the ground state and to the 2.211-MeV level. Thus, we consider in detail only the possibilities  $J=2$  or 3. We note also that the possibility  $J\leq 1$  had been previously excluded.<sup>4</sup>

A summary of the available correlation information is given in Table II, which lists for each transition the relative intensity measured at the three angles  $\theta_\gamma=37^\circ, 55^\circ, 90^\circ$ .

Figure 5 summarizes the results of a  $\chi^2$  analysis of the correlation data on the two strongest cascade transitions, as indicated in the inserts. Here we have plotted the goodness-of-fit parameter  $\chi^2$  versus  $x_1$ , the  $(L+1)/L$  mixing in the first member of each of the indicated cascades, for assumed values  $J=2, 3$  for the spin of the 3.52-MeV initial level. In both cases, the mixing in the second member is either identically, or approximately, zero.

Figure 5(a) shows the results for the  $3.52\rightarrow 1.95\rightarrow 0.58$

cascade. Here the  $E2/M1$  mixing in the second member has been previously restricted<sup>4,6</sup> to be  $+(0.04\pm 0.06)$  as indicated. Clearly acceptable solutions for  $x_1$  are obtained for both  $J=2$  and  $J=3$ , i.e., the value of  $\chi^2$  dips well below the 10% confidence limit for both cases. The restrictions on  $x_1$  (taken at the 1% confidence limit) obtained from this analysis are summarized in Table II. We note here that for  $J=3$  the analysis is consistent with the  $3.52\rightarrow 1.95$  transition being pure dipole.

The results of a similar analysis of the  $3.52(J)\rightarrow 2.21(1^-)\rightarrow 0.66(0^+)$  cascade transition are shown in Fig. 5(b). Here the second transition must be pure dipole. These results exclude the possibility  $J=2$  for the 3.52-MeV level, while for  $J=3$  they are consistent with the  $3.52\rightarrow 2.21$  transition being of pure quadrupole character.

We note that the selection of  $J=3$ , as opposed to  $J=2$ , is obtained only from a simultaneous fit to *all* the correlation data on the  $3.52\rightarrow 2.21\rightarrow 0.66$  cascade. Also given in Table II are the restrictions obtained on the  $(L+1)/L$  mixing for the  $3.52\rightarrow 0$ ,  $3.52\rightarrow 0.89$ , and  $3.52\rightarrow 2.57$  transitions obtained from independent fits to these data. As can be seen from the  $\chi^2$  values, these results jointly and independently establish a strong preference for a  $J=3$  assignment for the 3.52-MeV level, thus supporting the results obtained from the  $3.52\rightarrow 2.21\rightarrow 0.66$  analysis.

We now combine these results with the lifetime information in order to consider the possibilities for an even- or odd-parity assignment for this level, noting that the restriction  $\tau < 60$  psec corresponds to a restriction on the level width of  $\Gamma_\gamma > 11 \times 10^{-8}$  MeV. If  $J^\pi=3^+$ , then the  $3.52\rightarrow 2.21$  transition is almost pure  $M2$ . The

<sup>21</sup> D. H. Wilkinson, in *Nuclear Spectroscopy*, edited by F. Ajzenberg-Selove (Academic Press Inc., New York, 1960), Part B, p. 862 ff.



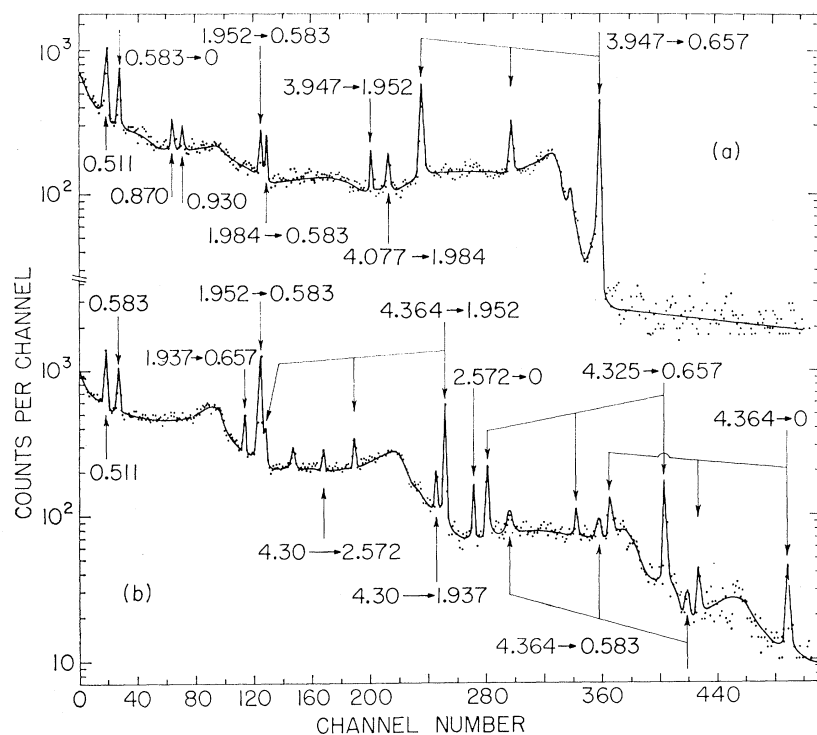


FIG. 7. Partial results of a two-parameter analysis of  $p$ - $\gamma$  coincidences in the  $\text{Ne}^{20}(\text{He}^3, p\gamma)\text{Na}^{22}$  reaction, illustrating the decay of levels of  $3.9 < E_{\text{ex}} < 4.4$  MeV. These data were measured with a 30-cc Ge(Li) detector with an intrinsic resolution of 3 keV, in coincidence with regions of proton pulse height corresponding (see Fig. 6) to channels (a) 20-24, and (b) 15-18, inclusive. The various lines are labeled according to the excitation energies (in MeV) of the  $\text{Na}^{22}$  levels between which the transitions occur. For the higher energy lines the positions of the first and second escape peaks, as well as the full-energy peak, are indicated. In (a), we see the principal decays of the 3.947- and 4.077-MeV levels, while in (b) we see the principal decays of the 4.325- and 4.364-MeV levels. Evidence for a previously unreported state at 4.30 MeV is illustrated, as explained in the text.

partial  $\gamma$  width corresponding to the measured branching ratio of  $22 \pm 3\%$  (to one standard deviation) is  $\Gamma_{\gamma}(3.52 \rightarrow 2.21) \geq 2.2 \times 10^{-3}$  meV. This corresponds<sup>21</sup> to a lower limit on the  $M2$  strength of  $\sim 5$  Weisskopf units (W.u.) which is unreasonably<sup>22</sup> large for a  $\Delta T=0$  transition in this, a self-conjugate, nucleus, and we thus reject an even-parity assignment for the 3.52-MeV level. Conversely, if  $J^{\pi}=3^{-}$ , the 3.52  $\rightarrow$  2.21 transition has an  $E2$  strength  $\geq 0.2$  W.u. which is quite reasonable. In conclusion, the 3.52-MeV state is found to have  $J^{\pi}=3^{-}$ . The branching ratios for the major decay modes have been summarized in Fig. 4. The results of the correlation analysis are consistent with the major transitions to the ground state ( $3^{+}$ ) and 1.952-MeV state ( $2^{+}$ ) being pure electric dipole, while that to the 2.211-MeV state ( $1^{-}$ ) must be electric quadrupole. The transition to the 2.57-MeV ( $2^{-}$ ) state may be a  $E2/M1$  mixture; the results indicate a nonzero  $E2$  component. The present results can be taken as reinforcing an odd-parity assignment for the 2.57-MeV level. For, if the 3.52  $\rightarrow$  2.57 transition were an  $M2/E1$  mixture, we would find an  $M2$  strength of  $>1$  W.u. which is unreasonably large for a  $\Delta T=0$   $M2$  transition in a self-conjugate nucleus. The transition to the 0.891-MeV state ( $4^{+}$ ) is expected to be pure  $E1$ , but the correlations place no restriction on a possible  $M2$  component.

<sup>22</sup> E. K. Warburton, in *Isobaric Spin in Nuclear Physics*, edited by J. D. Fox and D. Robson (Academic Press Inc., New York, 1966), pp. 90-112.

#### Results for the Higher-Lying States

Information on the  $\text{Na}^{22}$  levels of  $E_{\text{ex}} > 3.9$  MeV was obtained from the second measurement at  $E_{\text{He}^3} = 5.81$  MeV. Figure 6 presents a portion of the two-parameter data obtained for  $\theta_p = 55^\circ$ , and shows the particle spectra measured in coincidence with specific  $\gamma$  rays. The advantages of the Ge(Li) detector resolution are evident here, since it easily resolved the  $\gamma$  rays of energy 1.369 and 1.400 MeV which characterize respectively the deexcitation of the  $\text{Na}^{22}$  states at 1.952 and 1.984 MeV to the first excited state at 0.583 MeV. From Fig. 6, it is immediately clear that the  $\text{Na}^{22}$  states at 3.521, 3.947, 4.364, 4.594, 4.782, and 5.073 MeV decay by cascades through the  $J^{\pi}=2^{+}$  1.952-MeV level. Conversely, the states at 4.077 and 4.727 MeV, decay through the 1.984-MeV level. Also shown in Fig. 6 are portions of the proton spectra measured in coincidence with those  $\gamma$  rays which characterize the deexcitation of the 4.631- and 5.184-MeV levels of  $\text{Na}^{22}$ . Thus, it is evident that these data contain information on the  $\gamma$  decay of 11 of the 16 levels of  $\text{Na}^{22}$  which have been reported<sup>1</sup> to lie between excitation energies of 3.5 and 5.2 MeV. It is also evident that the particle detector is not able to resolve the structure in this region. What was done then was to examine the  $\gamma$  spectrum in coincidence with the 2 or 3 peak channels of a given proton group, utilizing the Ge(Li) resolution to determine the decay modes of that particular state. Finally, plots similar to Fig. 6 were

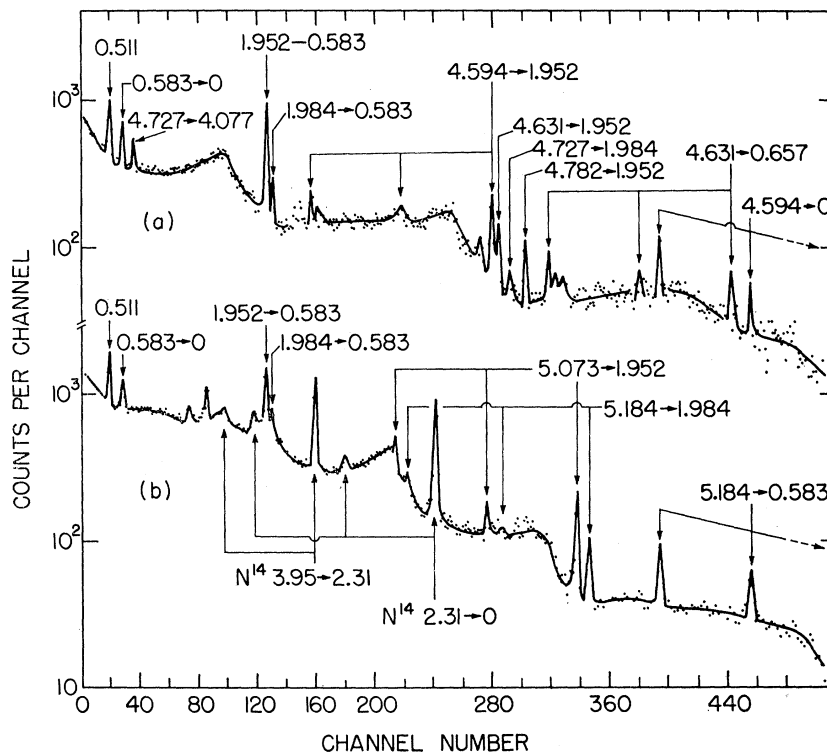


FIG. 8. Partial results of a two-parameter analyses of  $p$ - $\gamma$  coincidences measured in the  $\text{Ne}^{20}(\text{He}^3, p\gamma)\text{Na}^{22}$  reaction at  $E_{\text{He}^3} = 5.1$  MeV. The notation is the same as that of Fig. 7. These spectra were measured in coincidence with proton channels (a) 2-6 and (b) 10-13 as illustrated in Fig. 6. Thus, in (a) we see the principal decay modes of the 4.59-, 4.63-, 4.73-, and 4.78-MeV levels, and in (b) the decay of the 5.07- and 5.18-MeV levels.

constructed showing the particle groups coincident with the specific  $\gamma$ -ray line or lines as measured by the Ge(Li) detector, characterizing the decay of the particular state. In this way, the major assigned decay modes of each state were examined and cross checked. In the following then, we merely summarize the conclusions.

Figures 7(a) and 7(b) illustrate the  $\gamma$ -ray spectra measured in coincidence with proton pulses falling in the range of channels 20-24 and 15-18, respectively, in Fig. 6, showing the major decay modes of the four previously reported levels of  $\text{Na}^{22}$  in this range of excitation energy. Each of the  $\gamma$ -ray lines which could be assigned as being in coincidence with a specific proton group is identified according to the initial and final states between which the transition occurs. From the data obtained at the three angles of observation  $\theta_\gamma = 37^\circ$ ,  $55^\circ$ , and  $90^\circ$ , the Doppler shifts of the prominent  $\gamma$ -ray lines were extracted, and in a fashion analogous to that presented above for the 3.52-MeV level, were used to set limits on the mean lifetimes of the initial  $\text{Na}^{22}$  levels. We summarize the results by noting that for all of the levels of  $3.9 \leq E_{\text{ex}} \leq 5.2$  MeV which were observed in the present experiment, a lower limit  $\tau < 100$  psec was placed on the mean lives of the initial states. An exception is made for the 4.727-MeV state for which we determine only  $\tau < 800$  psec. We now consider the results for each level.

*The 3.947-MeV level.* The 3.947-MeV level is ob-

served to decay to the 0.657- and 1.952-MeV levels with branches of  $93 \pm 1\%$  and  $7 \pm 1\%$ , respectively. The branching ratios quoted here are an average of the measurements at  $E_{\text{He}^3} = 6.2$  and 5.8 MeV, which were in good agreement. They are also in excellent agreement with the values  $92 \pm 3$  and  $8 \pm 3$  reported previously.<sup>4</sup> Table III summarizes the results of these branching-ratio measurements, and gives also the upper limits which can be placed on unobserved transitions. The 3.947-MeV level has been previously assigned  $J=1$  from correlation studies in the  $\text{Ne}^{20}(\text{He}^3, p\gamma)\text{Na}^{22}$  reaction. The present correlation results confirm that assignment.

*The 4.077-MeV level.* As is evident from Fig. 6(a) the present results determine unambiguously that the 4.077-MeV level decays primarily to the 1.984-MeV level, which has  $J^\pi = 2^+$  or  $3^+$ . Branches to other states of  $\text{Na}^{22}$  are less than 25% of the main branch. This is in agreement with the previous<sup>2,4,11</sup> (but somewhat tentative) conclusions on the decay of this level. As pointed out previously,<sup>4</sup> identification of the 4.077-MeV level as  $J^\pi = 4^+$ ,  $T=1$  (as previously hypothesized) would establish a strong preference for a  $J^\pi = 3^+$  assignment for the 1.984-MeV level (as opposed to the  $2^+$  alternative).

*The 4.325- and 4.364-MeV levels.* The decay of these levels has been observed previously<sup>2,4</sup> with NaI(Tl) spectroscopy. The present results are in general agreement with the previously stated conclusions, but the

TABLE III. Summary of branching ratio information for states of  $\text{Na}^{22}$  of  $E_{\text{ex}} > 3.5$  MeV. Branching ratios are given (in percent) for transitions from the given initial states to the indicated final states. Unless otherwise stated, an upper limit of 25% can be placed individually on unobserved branches.

Final state ( $E_{\text{ex}}$ in MeV)	3.521 <sup>a</sup>	3.708 <sup>b</sup>	3.947 <sup>a</sup>	4.077	4.300	4.325	4.364	4.594	4.631	4.727	4.782	5.073	5.184
0	22±4		<1.3		<10	<5	18±3	30±10			<5	<10	<15
0.583	<3		<2		<10	<7	6±3	<10			<5	<10	45±10
0.657	<3		93±1		<10	100	<3	<10	40±12		<5	<10	<10
0.891	8±2	65±10	<2		<10	<6	<5	<10			<5	<10	<10
1.528	<3	35±10	<2		<10	<4	<5	<10			<5	<10	<10
1.937	<3		<2		60±10	<8	<5	<7			<7	<7	<10
1.952	40±5		7±1		<10	<9	76±4	70±10	60±12	60±10	100	100	<10
1.984	<3		<2	100	<10	<7	<7	<7			<7	<7	55±10
2.211	22±3		<2		<10	<6	<10	<10			<5	<10	<10
2.572	8±2		<2		40±10	<6	<10	<10			<7	<10	<10
2.969	<4		<2		<10	<6	<10	<10			<5	<10	<10
3.059	<4		<2		<10	<5	<10	<10			<5	<10	<10
3.521			<3		<10	<4	<10	<10			<10	<10	<10
3.708			<3		<10	<7	<10	<10			<10	<10	<20
4.077										40±10	<20	<20	<20

<sup>a</sup> Results quoted represent an average of the present results with those of Ref. 4.

<sup>b</sup> This level not populated in present experiment. Values quoted are from Ref. 4.

superior Ge(Li) resolution permits a more certain unraveling of the decays from these two levels, which were not resolved by the particle detector. The 4.325-MeV level is observed to decay only to the 0.657-MeV level; the upper limits which can be set on other possible decays are given in Table III.

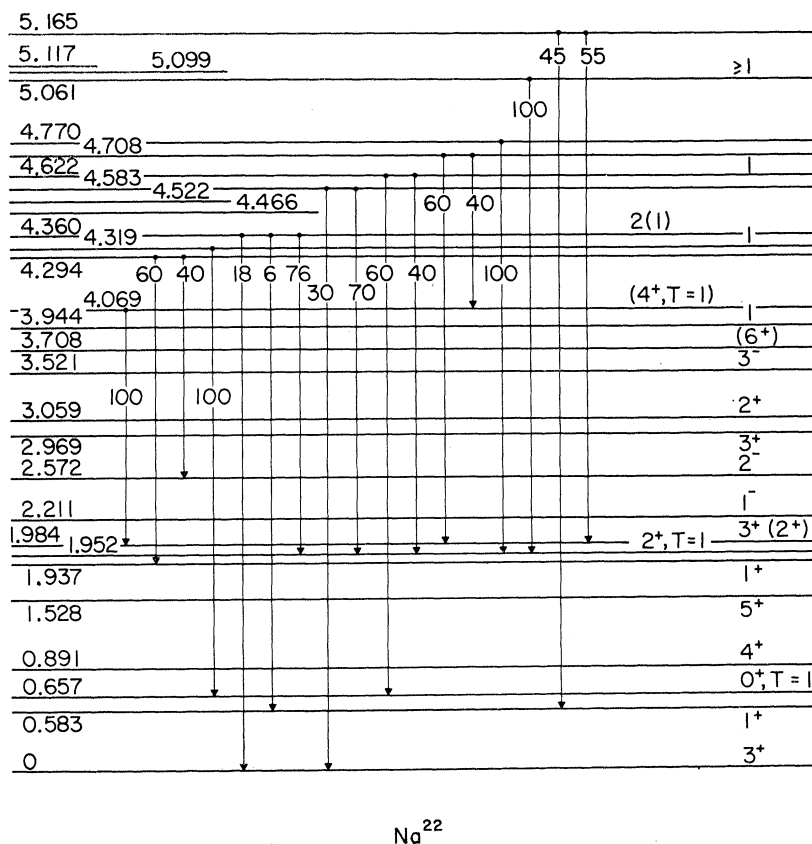
The 4.364-MeV level is observed to decay to the ground state and to the 0.583- and 1.952-MeV levels with the branching ratios indicated in Table III. The transitions indicated above arising from the decay of the 4.325- and 4.364-MeV levels account for most of the strong peaks in the spectrum of Fig. 7(b), with the exception, in particular, of lines at  $E_{\gamma} = 2.57, 2.36, 1.73,$  and 1.28 MeV. An examination of the proton spectrum coincident with these  $\gamma$ -ray peaks shows a proton group corresponding to an excitation energy in  $\text{Na}^{22}$  of  $4.30 \pm 0.01$  MeV. The observed transition energies and intensities fit well with such a level, which decays via the principal cascade transitions  $4.30 \rightarrow 2.572 \rightarrow 0$  and  $4.30 \rightarrow 1.937 \rightarrow 0.657$ . The existence of this previously unreported state, for which the evidence is quite conclusive, resolves the discrepancies between the branching ratios given above and those given previously<sup>4</sup> for the decay of the 4.325- and 4.364-MeV levels.

We note that the second escape peak of the  $4.364 \rightarrow 1.952$  transition has an energy which is barely distinguishable from that of 1.400 MeV resulting from the  $1.984 \rightarrow 0.583$  cascade transition. This "accidental" energy overlap explains the presence of the particle peak measured in coincidence with 1.40-MeV  $\gamma$  rays in Fig. 6. Table III summarizes the information obtained from this experiment on the  $\gamma$  branching of this triplet of states. The observed decay routes are illustrated schematically in Fig. 9, which also summarizes the results for the higher-excited states studied in the present experiment.

*Levels of  $4.4 < E_{\text{ex}} < 4.8$  MeV.* The  $\gamma$  spectrum coincident with particle channels 10-13 (Fig. 6) is shown in Fig. 8(a), and illustrates the major decay of 4 of the 6 states of  $\text{Na}^{22}$  lying in this region of excitation energy. No evidence was obtained for population of the states at 4.474 and 4.531 MeV. The results of Fig. 6 indicate that the 4.594-MeV level has a major branch to the 1.952-MeV level. The spectrum of Fig. 8(a) confirms this, and determines that the principal branches are to the ground state and to the 1.952-MeV level. The 4.631-MeV level decays to the 0.657-MeV level and to the 1.952-MeV level. Again, the coincident proton spectra of Fig. 6 shows that the  $\gamma$  ray of energy 2.68 MeV, corresponding to the  $4.631 \rightarrow 1.952$  transition, indeed arises from the 4.631-MeV level.

The results of Fig. 6 indicate that the 4.727-MeV level decays primarily to the 1.984-MeV level. However, the intensity of the  $1.984 \rightarrow 0.583$  peak [Fig. 8(a)] is too strong (by a factor of 2) to be attributed entirely to the  $4.727 \rightarrow 1.984 \rightarrow 0.583$  cascade transition. The difference arises from the  $4.727 \rightarrow 4.077 \rightarrow 1.984 \rightarrow 0$  cascade transition, which gives rise to the 0.635-MeV

FIG. 9. Summary of information on spins and parities for levels of  $\text{Na}^{22}$  of  $E_{\text{ex}} < 5.2$  MeV, incorporating the results of the present experiment. In particular, the assignments as well as the branching ratios for levels of  $E_{\text{ex}} > 4.1$  MeV are from the present report. The assignments of even parity for the 2.97- and 3.06-MeV levels, and the  $J = 3^-$  assignment for the 3.52-MeV level are also determined from the present set of experiments. Uncertain assignments, or alternatively those suggested from model predictions, are enclosed in parentheses.



$\gamma$  ray which appears in channel 35. The branching ratios are  $4.727 \rightarrow 1.984$  ( $60 \pm 10\%$ ) and  $4.727 \rightarrow 4.077$  ( $40 \pm 10\%$ ). The observed branching suggests a high spin for the 4.727-MeV level, since the 0.634-MeV transition to the 4.077-MeV state (suspected  $J^\pi = 4^+$ ) competes in this case favorably with the 2.743-MeV transition to the 1.984-MeV state (most probably  $J^\pi = 3^+$ ).

*Levels of  $E_{\text{ex}} > 4.8$  MeV.* The final piece of information on the decay of the higher-lying levels of  $\text{Na}^{22}$  is contained in Fig. 8(b), which illustrates the principal decay modes of the levels at excitation energies of 5.073 and 5.184 MeV. The 5.073-MeV level is observed to branch only to the 1.952-MeV level. The 5.184-MeV state decays to both the 0.583-MeV state and to the 1.984-MeV state.

Also present in the spectrum of Fig. 8(b) are the cascade  $\gamma$  rays from the 3.95-MeV state of  $\text{N}^{14}$ , formed through the  $\text{C}^{12}(\text{He}^3, p)\text{N}^{14}$  reaction due to carbon contamination of the Ni entrance foil. The presence in the two-parameter data matrix of  $p$ - $\gamma$  coincidences from the latter reaction provided in this case useful calibration points for the particle and  $\gamma$ -ray spectra.

The branching-ratio information for these higher-lying states has been summarized in Table III. The observed branches are indicated schematically in Fig. 9 which summarizes also the available information on the

spin/parity assignments for the levels of  $\text{Na}^{22}$  obtained from this and previous experiments.

### B. NaI(Tl) Correlation Information

As pointed out in the previous subsection,  $p$ - $\gamma$  angular correlation measurements for  $\theta_\gamma < 37^\circ$  were precluded by the design of the 5-in.-diam scattering chamber. This restriction, coupled with the statistical uncertainties due to the low coincidence count rates, resulted in relatively large errors in subsequent determinations of the  $P_4(\cos\theta)$  terms in Legendre polynomial fits to the correlation data. Therefore, a second set of measurements was undertaken using an 8-in.-diam chamber, with a  $3 \times 3$ -in. NaI(Tl) detector replacing the Ge(Li) detector. The NaI(Tl) detector was placed 15 cm from the target, and could be rotated in the region  $0^\circ \leq \theta_\gamma \leq 90^\circ$ . The annular particle detector subtended an angle of  $171 \pm 1.7^\circ$ , and was shielded against elastically scattered  $\text{He}^3$  particles by a 1-mil Al absorber. Measurements were carried out at a  $\text{He}^3$  bombarding energy of 6.2 MeV, which after correction for the energy loss in the target entrance window (0.05-mil Ni), corresponds to an energy incident on the  $\text{Ne}^{20}$  gas of 5.84 MeV. In other respects, the experimental apparatus was identical to that described in Sec. III A.

TABLE IV. Summary of  $(p, \gamma)$  angular correlation data from the  $\text{Ne}^{20}(\text{He}^3, p\gamma)\text{Na}^{22}$  reaction as measured at two different bombarding energies  $E_B$ . The Table shows the Legendre polynomial coefficients measured for the various indicated transitions from the given initial states ( $E_i$ ) and the corresponding goodness of fit parameters  $\chi^2$ . Allowed values of  $J_i$  and the restrictions on  $x$ , the  $(L+1)/L$  mixing in the primary transitions, are tabulated together with the minimum  $\chi^2$  obtained in these fits. The various final-state spins are 0.58 ( $J=1$ ), 0.66 ( $J=0$ ), 1.95 ( $J=2$ ).

$E_B$ (MeV)	$E_i$ (MeV)	Transition	$a_2$ (%)	$a_4$ (%)	$\chi^2$	$J_i$	$(L+1)/L$ mixing in primary transition from the given initial state	$\chi^2$ (fit)			
6.20 <sup>a</sup>	3.947	3.95→0.66	-37±2	0±2	1.0	1	$x=0$	1.0			
6.20 <sup>a</sup>	4.325	4.32→0.66	+16±5	0±5	0.7	1	$x=0$	0.7			
6.20 <sup>a</sup>	4.364 <sup>b</sup>	4.36→1.95	+35±5	-3±5	0.7	1	$x < -0.3$	$x = +(1.0 \pm 0.5)$	0.6		
		1.95→0.58	+1±4	-3±4	1.0			2	$x = -(2.2 \pm 1.0)$	$x = -(0.1 \pm 0.2)$	1.0
6.20 <sup>a</sup>	4.631	4.63→0.66	-36±4	-1±3	0.3	1	$x=0$	0.3			
6.20 <sup>a</sup>	5.073 <sup>b</sup>	5.07→1.95	+45±1	-1±10	1.4	1	$x < -0.7$	$x = +(0.67 \pm 0.33)$	0.9		
		1.95→0.58	-11±6	-6±5	1.9			2	$-0.45 < x < +0.3$	0.9	
								3	$x < -1.2$	$x = -(0.5 \pm 0.2)$	1.5
								(4) <sup>c</sup>	$x = +(0.0 \pm 0.2)$	2.7	
6.56 <sup>d</sup>	4.325	4.32→0.66	-51±8	+17±7	1.8	1	$x=0$	2.0			
6.56 <sup>d</sup>	4.364	4.36→0.58	-46±4	-13±4	2.8	(1) <sup>e</sup>	$-60 < x < -0.2$	$+0.4 < x < +2.6$	4.4		
								2	$x = +(0.27 \pm 0.09)$	$x = +(2.1 \pm 0.4)$	2.2
6.56 <sup>d</sup>	4.364 <sup>b</sup>	4.36→1.95	+49±4	0±6	0.1	1	$x < -0.8$	$x = +(0.65 \pm 0.22)$	0.7		
		1.95→0.58	-12±5	-13±6	0.8			2	$x = -(0.2 \pm 0.3)$	0.7	

<sup>a</sup> Present experiment.

<sup>b</sup> Restrictions on  $x$  were obtained from a simultaneous fit to both the indicated transitions. In these cases, the information contained in the second member of the cascade has been used to help fix the population parameters

of the initial state. It has been previously established that the 1.95(2<sup>+</sup>)→0.58(1<sup>+</sup>) transition is essentially pure dipole.

<sup>c</sup> The spin possibilities in parenthesis are considered less likely, as the minimal  $\chi^2$  exceeds the 1% confidence limit.

<sup>d</sup> Data of Ref. 4.

$p$ - $\gamma$  coincidences were stored in a two-parameter matrix of  $128(p) \times 128(\gamma)$  channels, with the range of analysis set to cover that given in Sec. III A. Correlation measurements were made at  $\theta_\gamma = 0^\circ, 30^\circ, 45^\circ, 60^\circ$ , and  $90^\circ$  with one angle repeated as a check on reproducibility. The data were acquired over a period of  $\sim 50$  h at a beam current of 70 nA, corresponding to a total bombardment of  $\sim 0.01$  C. An analysis of these data confirms the major decay modes summarized in Fig. 9 (and Table III) for levels at 4.30, 4.32, 4.36, 4.59, 4.63, 4.73, 4.78, 5.07, and 5.18 MeV. In particular the presence of the proton group corresponding to the 4.30-MeV state was clearly evident, yielding once more a value for the excitation energy of the state of  $4.30 \pm 0.01$  MeV.

The spectra obtained for each angle were analyzed, as described previously,<sup>4</sup> to obtain the angular dependence of the various deexcitation  $\gamma$  rays. These results were then fitted with an even-order Legendre polynomial expansion of the form of Eq. (1). In Table IV, we have summarized the results for those  $p$ - $\gamma$  correlations which could be unambiguously extracted from the data; i.e., in these cases the resolution of the  $\gamma$  detector/proton detector was sufficient to resolve the correlation of interest from near-lying coincidence peaks present in the two-parameter matrix. In these cases, we have also used the branching-ratio information of Table III to ascertain the reliability of the results. Values of  $\chi^2$  resulting from the Legendre polynomial fit to the cor-

relation data are given as well as the  $a_2$  coefficients. Also given in Table IV are some results from a previous experiment<sup>4</sup> performed at  $E_{\text{He}^3} = 6.56$  MeV, which we can now interpret since the decay schemes of the 4.32- and 4.36-MeV levels have been determined.

The correlation results summarized in Table IV were next analyzed to see what restrictions could be placed on the spins of the initial  $\text{Na}^{22}$  levels and on possible multipole mixings in the principal deexcitation  $\gamma$  rays. This was done by performing a  $\chi^2$  analysis for various assumed spins for each of the initial levels (as illustrated, for example, in Fig. 5); those spin possibilities for which the minimal values of  $\chi^2$  exceeded the 0.1% confidence limit were rejected.

Columns 7 and 8 of Table IV summarize our conclusions on the allowed spins for the initial levels and on the  $(L+1)/L$  mixing of the primary deexcitation  $\gamma$  transitions. The minimum values of  $\chi^2$  obtained in these fits are given in column 9, and may be compared directly to the values given in column 6. We now consider the results individually.

For the 3.95-, 4.32-, and 4.63-MeV levels, which decay to the 0.66-MeV state, the analysis is particularly simple. Since the 0.66-MeV level has  $J=0$ , the transitions to this state are pure multipoles, of character  $L = \Delta J = J_i$ . Thus the only explicit parameters of the fit are the unknown substate populations  $P(0)$  and  $P(1)$ . The possibility that  $J > 3$  for these states can be eliminated on the basis of the lifetime restriction given

previously that  $\tau < 100$  psec. Thus, we need consider only the possibilities  $J=1, 2, 3$ . For all three levels we obtain firm  $J=1$  assignments as indicated in Table IV.

For the 4.36-MeV level the observation of significant anisotropies in the deexcitation  $\gamma$  rays determine that  $J > 0$ . Since the lifetime restriction again insures that the transition to the  $J^\pi = 2^+$ , 1.95-MeV state has  $L < 3$ , we need consider only the possibilities  $J=1-4$ . The correlation results for the 4.36 $\rightarrow$ 0.58 transition exclude possibilities  $J=3$  and 4, since for these cases  $\chi^2$  considerably exceeds the 0.1% limit. For  $J=2$  the fit is reasonable, while for  $J=1$  the value of  $\chi^2$  exceeds the 1% limit, and is thus considered quite unlikely. For either case, the restrictions on the 4.36 $\rightarrow$ 0.58 quadrupole/dipole mixing ratio  $x$  are given.

The two sets of data on the 4.36 $\rightarrow$ 1.95 $\rightarrow$ 0.58 also exclude possibilities  $J=3$  or 4, thus this rejection is quite firm. For each set of data the restriction on  $x_1$ , the mixing ratio in the 4.36 $\rightarrow$ 1.95 transition is given. The mixing in the 1.95 $\rightarrow$ 0.58 has been previously established as  $x_2 = +(0.04 \pm 0.06)$ . Combining the results obtained at the two bombarding energies we have, for the preferred  $J=2$  assignment, the restriction on the 4.36 $\rightarrow$ 1.95 transition that  $x = +(0.1 \pm 0.2)$ ; that is, the results are consistent with the transition being a pure dipole radiation. For the significantly less likely assignment  $J=1$ , the restrictions are that  $x < -0.8$  or  $x = +(0.65 \pm 0.22)$ , i.e., the transition has a significant quadrupole component.

Also shown in Table IV are some results on the  $\text{Na}^{22}$  5.073-MeV level. Consideration of the lifetime limit,  $\tau < 100$  psec, and analysis of the correlation data restricts the spin of this level to  $J=1, 2, 3$ , or 4, with the latter considered rather unlikely. The restrictions on  $x$ , the mixing in the 5.07 $\rightarrow$ 1.95 transitions, are given for each possibility.

### C. Excitation Energies

In the foregoing presentation we have labeled the various transitions according to the excitation energies of the initial and final states given in Fig. 1. Having thus identified the lines evident in Figs. 4, 7, and 8, these data were then used to obtain more accurate values for the excitation energies of the higher-lying  $\text{Na}^{22}$  levels. Values for the transition energies were obtained from the data for  $\theta_\gamma = 90^\circ$ , for which case the Doppler shifts were zero, and also from the  $55^\circ$  and  $37^\circ$  data, utilizing the information that (within the experimental uncertainties) the various deexcitation  $\gamma$  rays all exhibit the full Doppler shift calculated for the reaction kinematics.

The energy calibration for these data was based on the previously reported<sup>3</sup> transition energies for  $\gamma$  rays originating from the states of  $E_{\text{ex}} < 3.1$  MeV, which have uncertainties of  $< 0.6$  keV. Thus, a calibration for the energy region  $E_\gamma < 2.4$  MeV utilized the previously quoted values for the 2.572 $\rightarrow$ 0, 1.984 $\rightarrow$ 0.583, 1.952 $\rightarrow$

TABLE V. Excitation energies (in keV) for  $\text{Na}^{22}$  states of  $3.5 < E_{\text{ex}} < 5.2$  MeV. With the noted exceptions the Ge(Li) results are from the present experiment.

From Hinds <i>et al.</i> <sup>a</sup>	From Ge(Li) measurements
3527 $\pm$ 10	3521 $\pm$ 2
3711 $\pm$ 10	3708 $\pm$ 1 <sup>b</sup>
3947 $\pm$ 10	3944 $\pm$ 2
4077 $\pm$ 10	4069 $\pm$ 2
...	4294 $\pm$ 2
4325 $\pm$ 10	4319 $\pm$ 2
4364 $\pm$ 10	4360 $\pm$ 2
4474 $\pm$ 10	(4466 $\pm$ 5) <sup>c</sup>
4531 $\pm$ 10	(4522 $\pm$ 5) <sup>c</sup>
4594 $\pm$ 10	4583 $\pm$ 2
4631 $\pm$ 10	4622 $\pm$ 2
4727 $\pm$ 10	4708 $\pm$ 3
4782 $\pm$ 10	4770 $\pm$ 2
5073 $\pm$ 10	5061 $\pm$ 2
5111 $\pm$ 15	(5099 $\pm$ 5) <sup>c</sup>
5132 $\pm$ 10	(5117 $\pm$ 5) <sup>c</sup>
5184 $\pm$ 15	5165 $\pm$ 4

<sup>a</sup> Reference 1.

<sup>b</sup> From Ref. 10.

<sup>c</sup> Not observed in the present experiment. Values are based on the extrapolation procedure explained in the text.

0.583, 1.937 $\rightarrow$ 0.657, and 0.583 $\rightarrow$ 0 transitions, as well as the  $\text{N}^{14}$  2.31 $\rightarrow$ 0 transition ( $E_\gamma = 2312.68 \pm 0.10$  keV)<sup>23</sup> and annihilation radiation ( $E_\gamma = 511.01 \pm 0.01$  keV).

Several of the higher-lying  $\text{Na}^{22}$  states were observed to decay by alternate cascade routes involving transitions of grossly different energies, thus permitting a calibration also for the region,  $E_\gamma > 2.4$  MeV. For example, the full-energy and one- and two-escape peaks of the 4.36 $\rightarrow$ 1.95 transition fall within the applicable range of the low-energy calibration for  $E_\gamma < 1.4$  MeV, thus establishing an accurate value for the transition energy and subsequently the excitation energy of the initial state. Thus, the 4.36 $\rightarrow$ 0 transition was used as a secondary calibration for the higher energy region.

Finally, a least-squares fit to all of the  $\gamma$ -ray energy calibration data was obtained using a polynomial representation  $E_\gamma = a + bx + cx^2$ , where  $x$  is the peak-channel number. For those states which decay by more than one cascade route, the excitation energies deduced for the initial states from the measured transition energies were found to agree within  $\pm 2$  keV, which is the over-all uncertainty we attach to these results.

Table V summarizes the values thus obtained for the excitation energies of these higher-lying  $\text{Na}^{22}$  states, and for comparison gives also the values of Hinds *et al.*<sup>1</sup>

<sup>23</sup> C. Chasman, K. W. Jones, R. A. Ristinen, and D. E. Alburger, Phys. Rev. **159**, 830 (1967).

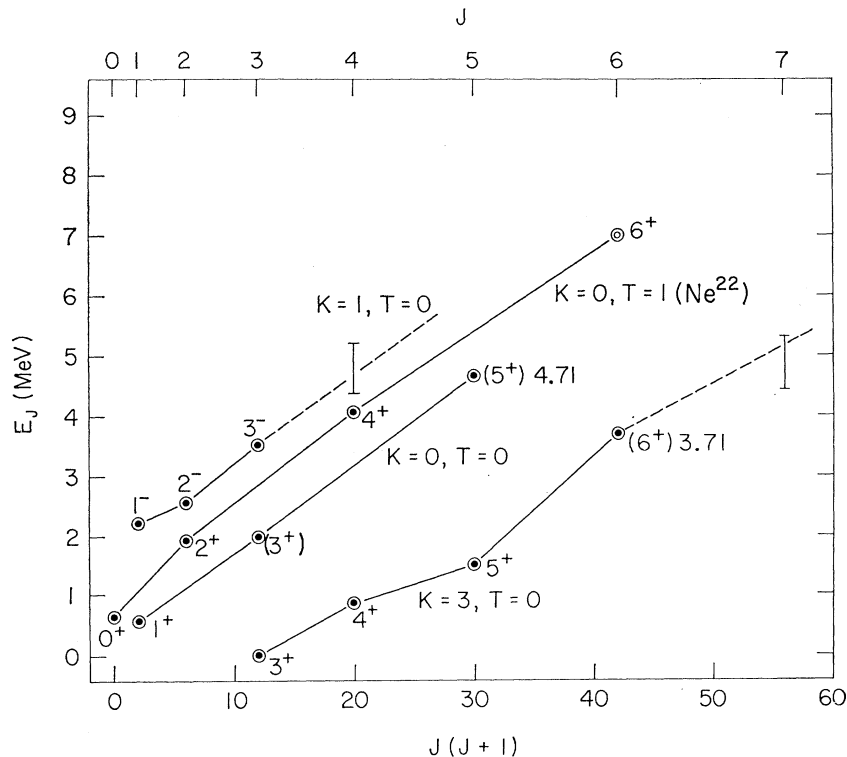


FIG. 10. Plot of excitation energies  $E_J$  (in MeV) for  $\text{Na}^{22}$  states with spin  $J$  versus  $J(J+1)$  for those levels which have been identified with the lowest-lying even- and odd-parity bands of  $\text{Na}^{22}$ , of the indicated intrinsic and isotopic spin ( $K, T$ ). The identification is outlined in Ref. 6. Spin/parity assignments which have not been rigorously determined, but only suggested, are enclosed in parentheses. Additionally, the  $(K, T) = (0, 1)$  band is that of  $\text{Ne}^{22}$  with the excitation energies increased by 0.66 MeV.

As can be seen, the agreement between the two sets of measurements is well within the quoted uncertainties of the two experiments. While the difference between the earlier results of Hinds *et al.* and those deduced in the present work became progressively larger with increasing excitation energy, it is evident that the former results give the level separations with considerably greater accuracy than the  $\pm 10$  keV assigned to the measured excitation energies. Therefore, we have used the results summarized in Table V to deduce the excitation energies also of the levels at 4.466, 4.522, 5.099, and 5.117 MeV, which were not observed in the present work. This was done by making a smooth fit to the excitation energies given in column 1 (of Table V) plotted as functions of the values given in column 2. The assigned uncertainties of  $\pm 5$  keV reflect the estimated errors in this procedure. Note that the excitation energies obtained in the present work are used in Fig. 9; while those of Hinds *et al.* are used for labeling the higher excited states in the earlier sections of this paper.

#### IV. DISCUSSION

One of the main aims of the present study was an identification of the  $3^-$  level of the  $T=0, 1^-, 2^-, 3^-, \dots$  rotational band of  $\text{Na}^{22}$ . It would appear that in this we were successful—the 2.969-MeV level was eliminated from contention and the 3.521-MeV level was found to have  $J^\pi=3^-$ . Proceeding under the assumption that

this is indeed an odd-parity rotational band, we note that the  $3.52 \rightarrow 2.21$  transition is an interband  $E2$  and should therefore be quite strong. If we take 30 W.u. as a reasonable upper limit on the strength of the  $3.52 \rightarrow 2.21$   $E2$  transition we obtain corresponding upper limits (in W.u.) on the observed  $E1$  transitions to the ground state, 0.891-, and 1.952-MeV level of  $1.5 \times 10^{-5}$ ,  $1.3 \times 10^{-5}$ , and  $31 \times 10^{-5}$ . Thus the  $E1$  decays of the 3.52-MeV level are all strongly retarded. A discussion of this retardation based on a preliminary analysis of the present work has been given.<sup>24</sup> A reasonable estimate of the  $3.52 \rightarrow 2.21$   $E2$  strength would be about 10 W.u., which is probably within a factor of 2 of the actual value. For this estimate the retardation of  $E1$  transitions would be  $\sim 3$  times greater than indicated above. The corresponding lifetime of the 3.52-MeV level would be 1.25 psec, which is accessible to measurement by the Doppler-shift attenuation method if one uses a solid stopping medium for the recoil  $\text{Na}^{22}$  ions.

Decay of the  $4^+$  level of the  $(K, T) = (0, 1)$  band to the ground state  $(3, 0)$  band by  $M1$  radiation is  $\Delta K$  forbidden; thus, this level is expected to decay mainly by an  $M1$  transition to the  $3^+$  level of the  $(0, 0)$  band. For this reason, the observed decay of the 4.069-MeV level to the 1.984-MeV level strongly supports the previous identification of these two states with the

<sup>24</sup> E. K. Warburton and J. Weneser, in *Isospin in Nuclear Physics*, edited by D. H. Wilkinson (North-Holland Publishing Co., Amsterdam, 1970), Chap. 5.

(0, 1)  $4^+$  and (0, 0)  $3^+$  states in question. These model-supported conjectures are indicated in Fig. 9.

Also indicated in Fig. 9 is the conjecture that the 3.708-MeV level is the  $6^+$  level of the (3, 0) band. Not indicated is the weaker possibility that the 4.708-MeV level is the  $5^+$  member of the (0, 0) band. These sup-

positions are illustrated schematically in the  $E_J$  versus  $J(J+1)$  plot of Fig. 10. This plot also indicates estimated excitation energies for the  $4^-$  level of the odd-parity band and the  $7^+$  member of the ground-state band. Clearly, further work is possible and desirable for an understanding of the collective states of mass 22.

## Gamma Rays Following Resonant Neutron Capture in $^{56}\text{Fe}^\dagger$

R. E. CHRIEN, M. R. BHAT, AND O. A. WASSON  
*Brookhaven National Laboratory, Upton, New York 11973*  
 (Received 28 October 1969)

The spectrum of  $\gamma$  rays following neutron capture at the 1167-eV resonance in  $^{56}\text{Fe}$  has been measured at  $90^\circ$  and  $135^\circ$  to the incident beam. The partial widths for radiative decay have been determined and compared to the Weisskopf estimates. The  $M1$  and  $E1$   $\gamma$ -ray strengths are found to be comparable, and a sizable  $E2$   $\gamma$  ray in the resonance has been recorded. On the basis of the  $\gamma$ -ray measurements at two angles, and from what has been determined from other experiments, the spin and parity of the 1167-eV resonance are shown to be  $\frac{1}{2}^-$ .

**T**HE lowest-energy neutron resonance in  $^{56}\text{Fe}$ , located at 1167 eV,<sup>1</sup> has been investigated by means of virtually all the techniques available to slow-neutron spectroscopy. This resonance thus serves as an excellent example of the combining of these techniques to completely determine the parameters of a neutron resonant state. The present paper is a description of a high-resolution  $\gamma$ -ray study of this level recently undertaken at the HFBR fast-chopper time-of-flight facility. The additional information gained by this study has led to a unique spin assignment for this level, as well as a determination of many of its partial radiative widths.

Because of its small neutron width, this resonance was not seen in earlier transmission studies. In 1960, however, Isakov, Popov, and Shapiro<sup>2</sup> reported its detection by measuring the energy dependence of the capture cross section in iron, using a lead "slowing down time" spectrometer. In 1963, Moore, Palevsky, and Chrien<sup>3</sup> determined the neutron and total radiation widths through the use of a self-indication method in conjunction with the Brookhaven National Laboratory-Atomic Energy of Canada, Ltd. Chalk River chopper. They also examined the resonance  $\gamma$ -ray spectrum with a low-resolution NaI detector and re-

ported a qualitative similarity between resonance and thermal capture in  $^{56}\text{Fe}$ .

High-resolution transmission data for this resonance were reported by Block<sup>4</sup> in 1964. The symmetry of the transmission dip with respect to its resonant energy led Block to conclude that the level was not due to  $S$ -wave neutron capture. Recently, Asami, Moxon, and Stein<sup>5</sup> have examined the scattered neutrons in an energy region containing this level as a function of energy and angle with respect to the incident beam. The appearance of an energy asymmetry in the differential cross section, and the angular behavior of that scattering-cross-section asymmetry enabled them to show that the resonant state is of odd parity.

In an effort to complete the specification of this state, the  $\gamma$ -ray spectra following the capture of neutrons in iron from thermal to  $\sim 2$  keV have been recorded with the aid of a two-parameter (neutron flight time and  $\gamma$ -ray detector pulse height) recording system and the HFBR fast chopper. A Ge(Li) detector of 4-cm<sup>3</sup> volume and with 0.1% energy resolution was used in the study. The  $\gamma$ -ray energies were measured relative to the  $^{54}\text{Cr}$  transition energies<sup>6</sup> and the hydrogen capture line,<sup>7</sup> and are believed to possess an absolute accuracy of better than 1 keV for  $6.5 \leq E_\gamma \leq 8.0$  MeV and better than 2 keV for  $E_\gamma \leq 6.5$  MeV, except for

<sup>†</sup> Work supported by the U.S. Atomic Energy Commission.

<sup>1</sup> *Neutron Cross Sections BNL 325* (U.S. Government Printing Office, Washington, D.C., 1966), 2nd ed., Suppl. 2.

<sup>2</sup> A. I. Isakov, Yu. P. Popov, and F. L. Shapiro, *Zh. Eksperim. i Teor. Fiz.* **38**, 989 (1960) [English transl.: *Soviet Phys.—JETP* **11**, 712 (1960)].

<sup>3</sup> J. A. Moore, H. Palevsky, and R. E. Chrien, *Phys. Rev.* **132**, 801 (1963).

<sup>4</sup> R. C. Block, *Phys. Letters* **13**, 234 (1964).

<sup>5</sup> A. Asami, M. C. Moxon, and W. E. Stein, *Phys. Letters* **28B**, 656 (1969).

<sup>6</sup> M. Mariscotti, W. R. Kane, and G. T. Emery, Brookhaven National Laboratory (private communication).

<sup>7</sup> R. C. Greenwood and W. W. Black, *Phys. Letters* **21**, 702 (1966).